12 Entropy Production in the Planetary Context

Ralph D. Lorenz

Lunar and Planetary Laboratory, University of Arizona, Tucson, AZ 85721, USA.

Summary. In this paper I review some applications of nonequilibrium thermodynamics to planetary science. Of particular importance are the horizontal and vertical transports of heat in planetary atmospheres. It has been noted that Titan and Mars, like the Earth, appear to have equator-to-pole heat transports consistent with a Maximum Entropy Production principle. The transport of heat by convection in the atmospheres and interiors of the planets can be viewed in heat engine terms, and useful insights gained by considering the irreversibilities in these systems. Even bodies in space without an atmosphere can act as heat engines, their orbits being modified by the Yarkovsky effect wherein sunlight is downconverted into thermal radiation which is reradiated anisotropically – a rocket using thermal photons as propellant. Finally, spacefaring civilizations may seek to maximize the production of entropy from their parent stars by erecting a Dyson sphere in order to reject its power at a minimum temperature.

12.1 Equator-Pole Temperature Gradients of Planetary Atmospheres

Planets are objects that intercept low-entropy energy as sunlight (short wavelength and unidirectional) and reradiate it in a higher-entropy form (as longer wavelength heat, and in many directions, e.g., Aoki 1983). Because planets are round, high latitude regions receive less sunlight than the tropics except for planets with high obliquities, when the opposite is the case. On an airless body, there is no heat transport and therefore show a substantial equator-to-pole temperature gradient and the planet is everywhere in radiative equilibrium. Planets with significant atmospheres (and oceans) permit significant heat flows which follow, and therefore mitigate, the temperature gradient. Were this heat flow performed with a near-infinite conductivity (or diffusivity) the planet would be isothermal.

As noted by Paltridge(1975) and in other chapters in this volume, the Earth's zonal climate can be reproduced remarkably well by assuming that these heat flows maximize the production of entropy. Simply put, if the heat flow F from tropical regions at temperature T_0 to cooler polar regions at T_1, the quantity $dS/dt = F/T_1 - F/T_0$ is maximized. Lorenz (1960) had noted before a related and essentially equivalent observation, that the Earth's climate maximizes the generation rate of Available Potential Energy (APE).

A. Kleidon and R.D. Lorenz (Eds.): Non-equil. Thermodyn., UCS 2, pp. 147–159, 2005.

Many papers discussing the application of MEP note that the generality of the principle should allow it to apply to other planetary bodies, and indeed since the coincidence of the observed terrestrial climate state with one of MEP might be just that, coincidence, an evaluation of the principle on other planets would be an independent test of the applicability of MEP. For this purpose, Lorenz et al. (2001) presented a simple two-box model that captures the essence of climate on a round planet (similar to the one used in the introductory chapter, Kleidon and Lorenz, this volume). A low and high latitude zone each receive different amounts of sunlight, each reject heat as a function of their temperature, and heat is transported between the two boxes depending on an effective heat diffusivity D. By varying D, the effect of heat transport on entropy production and the equator-pole temperature gradient of different planetary atmospheres can be investigated.

12.1.1 Earth

For the present-day Earth, the insolation I_0 in the low-latitude box is about $I_0 = 240\,W\,\mathrm{m}^{-2}$, taking into account the albedo, while at higher latitudes we have $I_1 = 140\,W\,\mathrm{m}^{-2}$. Heat leaves the planet as thermal radiation from the two zones, with the outgoing emission related to temperature by $E_x = A + B\,T_x$. In the grey atmosphere approximation, $B \sim 4\sigma T^3/(1 + 0.75\tau)$, with τ being the infrared optical depth and σ being the Stefan-Boltzmann constant. Earth has an optical depth of about $\tau \sim 4$ and $T \sim 290\,\mathrm{K}$, so $B \sim 2\,\mathrm{W\,m^{-2}\,K^{-1}}$. (Lorenz et al. (2001) use a 'false' $\tau = 0.9$ in order for the grey radiative approximation to yield the correct surface temperature, but of course the atmosphere is actually in radiative-convective equilibrium, not in purely radiative equilibrium, and the real opacity is around 4. The real opacity yields an estimate for B that is closer to the empirical one from satellite observations.) If heat is transferred between the boxes at a rate $F = 2D(T_0 - T_1)$, then it is easy to show that the temperature difference ΔT is given by $\Delta T = T_0 - T_1 = (I_0 - I_1)/(B + 4D)$. For this formulation the entropy production dS/dT has a maximum for $D = B/4$, i.e., ~ 0.5–$0.8\,\mathrm{Wm^{-2}\,K^{-1}}$ – similar to observed values and leading to a temperature gradient consistent with observations (Fig. 12.1a). Somewhat equivalently, in the absence of atmospheric opacity effects, it emerges that the observed temperatures require D to have a numerical value close or equal to, the planet's average entropy production I/T.

12.1.2 Titan

Saturn's cold atmosphere-shrouded moon Titan has a thick, slowly-rotating atmosphere which exhibits a surprisingly large brightness temperature contrast of about 3 K compared with an equatorial temperature of about 93 K. Lorenz et al. (2001) noted that the observed brightness temperature contrast is exactly what would be predicted from MEP. Zonal models using mass-scaled D of 10^2 $-10^3\,\mathrm{W\,m^{-2}\,K^{-1}}$ predict contrasts of around 0.01 K. In contrast, the MEP principle mandates a D value rather lower than Earth of about $D \sim 4\sigma(93)^3/(1+0.75\tau)$ or around $0.02\,\mathrm{Wm^{-2}\,K^{-1}}$, leading to temperature contrast of a few K as observed (Fig. 12.1b). It is not clear how Titan's apparent heat transport is so inefficient. It may be that the latitudinal winds are suppressed by the strong zonal wind field, or that a condensation/evaporation phenomenon pins the polar temperatures at a low value. However, the *prima facie* agreement of the principle with the observed temperatures on Titan lends strong support to the MEP principle although some uncertainty regarding a possible stratospheric contribution to the brightness temperatures exists.

12.1.3 Mars

Lorenz et al. (2001) also consider the atmosphere of Mars. At first look, Mars does not obey MEP – its climate can be largely reproduced with the very small heat transport expected in a thin atmosphere (i.e., $D < 0.01\,\mathrm{W\,m^{-2}\,K^{-1}}$). However, its winter poles would get too cold with this value of D, and models are forced to pin them at the CO_2 condensation temperature of around 150 K. This is a quite reasonable 'fix' to the models, given that we can observe this process in action with the seasonal growth and

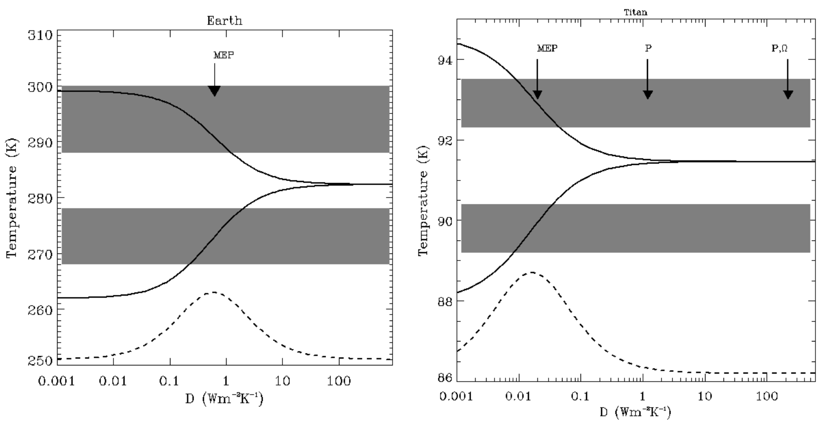

Fig. 12.1. Observed (*shaded boxes*) and modeled low and high latitude annual mean temperatures (*upper* and *lower lines* respectively). Simulated temperatures are a function of the heat transport parameter D. Entropy production (*dashed curve* – arbitary units) peaks for the Earth where the model curves agree with observations. On Titan, the entropy production curve again peaks (MEP) for the heat transport required to match observed temperatures, whereas pressure (P) and pressure/rotation rate scaling of the terrestrial values (P, Ω) fail, predicting temperature contrasts that are much too low. Adapted from Lorenz et al. (2001) and Ozawa et al. (2003)

decay of CO_2 frost caps. However, when the latent heat transport from the condensing cap to the atmosphere thence to the subliming cap is taken into account, the heat flow is entirely consistent with what would be predicted from MEP, of around $4\sigma(200)^3/(1 + 0.75\tau)$ or $\sim 0.4\,\mathrm{W m^{-2}\,K^{-1}}$. Were meteorologists unaware of the CO_2 condensation, the predictions of GCMs or zonal models would be gravely in error, yet only knowledge of the basic radiative setting of the planet (insolation, obliquity, albedo and IR opacity) allows MEP to correctly predict that the atmosphere does *something* to ensure a heat transport of $\sim 0.4\,\mathrm{W m^{-2}\,K^{-1}}$, corresponding to $\sim 1\,\mathrm{m}$ of seasonal frost and winds of several $\mathrm{ms^{-1}}$, as observed. This underscores the potential utility of MEP for astrobiological studies in predicting the resultant climate state, even when all the contributing mechanisms are not known.

12.1.4 Venus

On hot Venus, temperature contrasts are believed to be quite low although there are no accurate measures of surface temperature with latitude. Both, MEP and more conventional pressure-scaling of heat transport coefficients give more-or-less equivalent results. While Venus may indeed obey MEP, it is not an ideal test case. Furthermore, it may be that the altitudes at which solar flux is absorbed and re-emitted need to be considered as well.

12.1.5 Other Planets

The rapidly-rotating giant planets deserve further attention from a thermodynamic perspective. An additional degree of freedom that these bodies have is the significant heat flow from the interior, which can be of the same order as, or even exceed, the absorbed solar flux. The planet Jupiter, for example, has near-zero obliquity and therefore has a strong equator-to-pole insolation gradient, but the heat flux from the interior can be biased towards the polar regions in order to offset this gradient. Thus horizontal heat transport from low to high latitudes need not occur and indeed, the strongly belted structure of the atmosphere suggests that large-scale meridional motions in the troposphere are weak, as might be expected from the dynamical perspective of a large, rapidly-rotating planet. An additional question that exists for all planets, but has been largely ignored, is whether MEP applies to the surface, or some integrated absorption and emission of energy in the atmosphere, or only at some specific levels in the atmosphere. For the giant planets where there is no surface, this question becomes crucial. In passing, we should also note the information-theoretic application of maximum entropy principles to circulation on Jupiter by Sommeria (this volume).

12.1.6 Other Processes in Planetary Atmospheres

It may be that vertical convection in planetary atmospheres acts to extract work from the radiative setting in a very analogous way to the horizontal heat transport discussed earlier in this chapter. Ozawa and Ohmura (1997) showed how a simple 1-D radiative-convective model, where an initial radiative solution is perturbed by an arbitrary convective flux versus altitude, yields a vertical temperature profile very much like that observed on Earth. The magnitude of the convective flux is similarly consistent with observations. This approach is rather different in philosophy from, but perhaps more generally applicable than, the usual technique of pinning the lower atmosphere to some critical lapse rate, which is somewhat arbitrarily chosen. On Earth, the value most commonly observed is 6.5 K/km, intermediate between the dry adiabat of ~ 9.8 K/km and a moist adiabat of around 5 K/km. This 'convective adjustment' approach has proven popular, since by definition it yields the observed result on this planet. It might be argued, however, that the entropy production maximization technique suggested by Ozawa and Ohmura (1997) involves fewer ad-hoc assumptions.

Lorenz and McKay (2003) explore grey models with imposed lapse rates, and determine in the conventional way the resultant convective flux required to yield the imposed temperature profile. This is the conventional procedure, although the fluxes are rarely reported, particularly over such a wide range of opacities. They find that convection acts as if it 'short-circuits' a resistance to upward transport of heat (i.e., opacity). The convective flux – analogous to an electrical current through a motor wired across a radiative 'resistor' in an electrical circuit – varies as if the motor adjusted itself to maximize the electrical power dissipated within itself.

Finally, Verkley and Gerkema (2004) note that under the constraints of maximum entropy and constant integrated thermodynamic temperature, a vertical atmosphere in a gravitational field is isothermal, while under constraints of maximum entropy and constant integrated potential temperature, the isentropic (i.e., adiabatic) profile is obtained. Yet if all three constraints are applied simultaneously in a variational manner, the resulting profile has a weaker lapse rate than the dry adiabat, and in fact rather closely resembles the lapse rate observed on Earth.

12.2 A Probabilistic Explanation for MEP

A persistent difficulty with MEP has been the lack, until Dewar's work (2003, also this volume), of a persuasive rationale for why a system like the climate should choose an MEP state. This can be explained as follows. The work output of the system is governed by the combination of heat flow and the Carnot efficiency for that heat flow, and thus is a curve that asymptotes to zero at low and high ($\Delta I/2$) heat flows, with an intermediate maximum. For the system to be in steady state, the frictional dissipation must balance out the work production.

We may consider the circulation as the combination of many flow modes, each of which is characterized by a certain amount of heat transport (F_i), and a certain amount of loss by frictional dissipation (L_i). These modes may be very efficient in the sense of having low L/F – a large-scale ocean current, for example, or very inefficient (high L/F) like a small-scale eddy. The aggregate heat transport of the system is simply $F = \Sigma F_{\rm i}$, and the dissipation $L = \Sigma L_{\rm i}$. At steady state, work output and dissipation are balanced, and thus $L \leq F\,\Delta T/T$.

If we presuppose that the system has many modes available that can combine to satisfy these constraints, then it follows that there are many more possible microscopic combinations of modes that yield a macroscopic steady state when that steady state has a higher value of dissipation and work output (along the lines of Dewar's interpretation of MEP, see also related discussion on fluid turbulence in Sommeria, this volume, and spatial degrees of freedom in atmospheric turbulence in Ito and Kleidon, this volume). If all possible combinations are populated with equal probability, then the most likely states are those with higher dissipation.

If the system does not have sufficiently different modes available to attain MEP, for example if all L_i are so large as to exceed $F\,\Delta T/T$, then clearly MEP cannot be a steady state. The system would seize up. An example of this situation is a rapidly-rotating planet, where the dynamic constraints on fluid motion suppress large-scale eddies, forcing instead higher-vorticity, and thus more dissipative, modes. Similarly, a thin atmosphere with a low column mass cannot hold or transport much heat without requiring very high windspeeds and thus friction.

Hence MEP for a planetary climate is a probabilistic result – it is likely, but not guaranteed and subject to the dynamical constraints of the system. The framework above allows us to consider the often-expressed but vague condition for MEP of requiring 'sufficient degrees of freedom to choose a macroscopic MEP state'. Sufficient degrees of freedom for a system can be interpreted here as having sufficiently different modes such that combinatorial statistics favour the macroscopic states of maximum power.

12.3 Dissipation and Heat Transport

Besides the dissipation of energy by the motion in planetary atmospheres, there are also other important contributions to the entropy budget of a planet. While simulations of a dry atmosphere indicate that around 70% of the dissipation is due to mixing and the dilution of heat, and only 30% is due to frictional dissipation, recent studies by Pauluis and Held (2002a,b) describe how the dominant entropy source in the real terrestrial atmosphere is the irreversibility due to moist processes (see also Goody (2000); Pauluis, this volume). At the microscopic scale, evaporation leads to locally saturated air. Thus any air of relative humidity less than 100% implies that mixing has occurred, by diluting the locally saturated air just above the condensed phase with dry air from elsewhere. This mixing is irreversible in the sense that it leads to entropy generation.

In gross terms, the Martian atmosphere transports a global, annual average of some $25\,\mathrm{W\,m^{-2}}$ of heat. This heat is transported over a substantial temperature difference, which in principle should lead to substantial Carnot efficiencies $\Delta T/T$ of 25% , and thus significant mechanical work – indeed rather comparable with that performed by the Earth's atmosphere. And yet, observations of Martian sand dunes, for example, show that they do not move, whereas terrestrial sand dunes move at up to several tens of meters per year.

The paradox is then, how can the Martian atmosphere transport so much heat, yet do so without producing a commensurate amount of work? Unless purely mechanical considerations (cementing of the dunes, or some mechanical coupling inefficiency in the thin atmosphere) are responsible, the answer is likely to lie in the entropy generation associated with the Martian frost cycle and irreversibilities from the phase changes involved.

Certain small-scale 'dry' processes lack the entropy production associated with phase changes, and an idealized Carnot heat engine model can yield impressively accurate predictions: a notably successful application is the modeling of Martian dust devils (Rennò et al. 2000).

However, large-scale transports are dominated by the frost cycle, and thus the phase-change irreversibilities are likely to play an important role in limiting the efficiency of the Martian heat engine. Fig. 12.2 shows the instantaneous radiative entropy fluxes on Mars from a Global Circulation Model showing the important contribution of the frost cycle to the overall entropy production. Infrared observations from the Mars Global Surveyor satellite may permit a study of the martian entropy budget much as was done for the Earth (e.g., Stephens and O'Brien 1993) in the 1970s and subsequently from the Nimbus-7, ERBE and other satellites.

Conrath and Gierasch (1985) note another phase change responsible for entropy production and limitation of the efficiency of the atmospheric heat engine, namely the ortho:para hydrogen transition of molecular hydrogen, which is the dominant constituent of the outer planet atmospheres. The ortho:para ratio at thermodynamic equilibrium is a function of temperature, but has a finite relaxation time. Thus large circulations may, for example, bring gas from depth more quickly than the relaxation time and introduce disequilibrium concentrations of para hydrogen. Since the ortho:para ratio can be determined from the speed of sound, or remotely by infrared spectroscopy, this disequilibrium may serve as a useful tracer of vertical motions. Another disequilibrium process that leads to significant dissipation in the atmosphere is the frictional dissipation around falling raindrops (e.g., Lorenz and Rennò 2002; Pauluis, this volume).

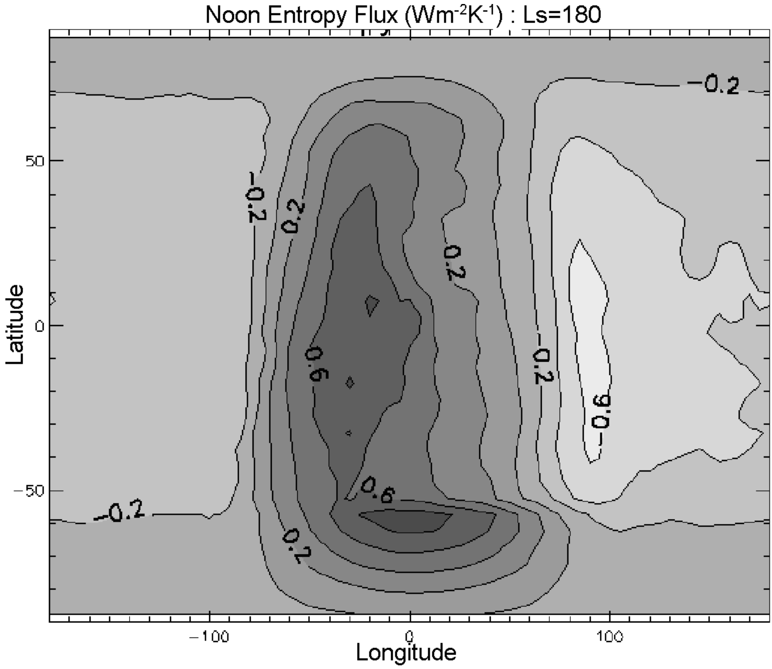

Fig. 12.2. Entropy Budget of Mars at L_s=180 using synthetic data from the European Mars Climate Database (available at http://www-mars.lmd.jussieu.fr/mars/access.html). Close to local noon (longitude 0), the budget is positive at around 0.6 $\mathrm{W m^{-2} K^{-1}}$ as the surface is absorbing heat. It falls sharply in the early evening to a similar, but negative value, as the surface rejects heat it has accumulated during the day. Note that the southern frost cap (extending south of 60°S at this season) has a substantially positive entropy budget as radiates far less heat than it receives. Because its temperature is still pinned by CO2 frost, the cap edge has the highest entropy production of over 0.8 $\mathrm{W m^{-2} K^{-1}}$ – the entropy budget has different information than simply the net flux

12.4 Geomorphology and Dissipative Structures

States of MEP can lead to highly organized, self-similar structures (see e.g., discussion on self-organized criticality and how it relates to MEP in Dewar, this volume). While some geomorphic structures on planets such as impact craters or volcanoes are the result of instantaneous catastrophic events, many other geological processes occur in settings where self-organization can occur: examples that have been suggested in the context of MEP are mantle convection (Vanyo and Paltridge 1981), sand dunes, and sorted stone circles (see also Ozawa et al. 2003).

Sand dunes are created by, and enhance, the exchange of momentum between the atmosphere and the ground. Their regular structures point to self-organization and Werner (1995) has noted that they are an ‘attractor’ –

initial distributions of sand over a surface in a simple model tend to converge to a state with dunes of a common form, dictated by the wind distribution and the sand supply. The hypothesis has been made that sand dunes may organize to optimize the sand transport normal to the dune crest. This concept may be directly analogous to one of Maximum Dissipation in that sand transport relates to the second or third power of shear velocity – the dune field may represent a sand system that has organized itself to maximally dissipate kinetic energy from the wind field while retaining a persistent organized form.

Another striking self-organized landform is the sorted circles that form in some frozen terrain. The circles, around a meter across, are formed from coarse stones that are segregated from the rest of the soil by repeated freeze-thaw cycles. (Kessler and Werner 2003) describe features in Alaska and Spitzbergen, where the observed morphology of the patterned ground (a labyrinth, or stripes, or circles etc.) depends on the stone:soil ratio, the surface slope and other parameters.

The role of entropy and thermodynamics in landscape processes was noted by Leopold and Langbein (1962): in particular the application of these ideas to river networks has received much attention in more recent years – see Miyamoto et al. (this volume) for more detailed discussion.

12.5 The Yarkovsky Effect – Migration of Meteorites via a Photon Heat Engine

In the 1990s, as both the Mars meteorite ALH84001 demanded attention to the migration of small bodies in space, and as telescopic surveys began to systematically inventory the population of small earth-crossing asteroids, a subtle effect has come to the fore in astrodynamics, now known as the Yarkovsky effect after a Polish engineer who discussed it around 1900 (but whose work has since been lost, see e.g., Farinella et al. 1998). This effect can be understood by noting that every photon has a tiny amount of momentum. If the photon is absorbed, or reflected, by a surface, then the surface must absorb, or reverse respectively, the momentum of the photon, and in so doing receives the momentum from it (or double, in the case of reflection). Thus a surface exposed to the sun experiences a momentum flux, a radiation pressure. This small force affects small particles with large area:mass ratios and is responsible for comet dust tails pointing away from the Sun and is the basis of ‘solar sailing’ (see also Burns et al. 1979).

But just as the short wavelength, high energy photons of sunlight exert a radiation pressure, so do the infrared photons associated with thermal emission, albeit less momentum per photon. Launching the photons exerts a small pressure, just as absorbing them does. So a hot surface experiences a small pressure, but a slightly larger pressure than a merely warm one. Yarkovsky realized that a body with an uneven temperature distribution would experience an uneven pressure, and hence a net force in space. A static body would of course be hottest on its sunlit side, and therefore experience a net force away from the sun due to the flux of thermal photons from that side. Consider an object in a circular orbit moving at right angles to the sun vector and with its axis of rotation orthogonal to the orbital plane (Fig. 12.3). If the body is rotating very slowly, the temperature has a strong noontime peak, exerting a radiation pressure away from the sun. But since the body is moving orthogonally to the radiation pressure force, the force performs no work on the body and its orbit does not change. On the other hand, if the body rotates quickly, the heat from the sun is smeared out over all angles, or, equivalently, all local times. The radiation pressure in all directions cancel out so there is no net force. At some intermediate rotation rate there is still a significant temperature bulge, but slewed round to the afternoon. There is thus still a net thrust, with a component along the object's direction of motion. Work is therefore done on the body, and its orbital energy increases (note the conceptual similarity with the climate model earlier). There are some variations on the Yarkovsky effect, depending on the eccentricity and inclination of the orbit, and the angle between the rotation axis of the asteroids and its orbital axis, but these are not be discussed here.

Lorenz and Spitale (2004) applied a thermodynamic analysis to the Yarkovsky effect. They noted that a simple linearized expression for the Yarkovsky force (e.g., Burns et al. 1979) may be written as $F_y = (8/3)\pi R^2 (\sigma T^4/\mathrm{c})\ (\Delta T/T)$. Since the input power is $\sim 4\pi\, R^2\ (\sigma T^4)$ and the work being done on the body moving at orbital speed v is vF_y it follows that the conventional engineering efficiency is $\sim (2/3)(\Delta T/T)\ (v/c)$. This can be seen as the product of a Carnot efficiency and a propulsive efficiency (v/c), a common term in rocketry, where the exhaust velocity of the propellant, here the speed of light c, should be matched to the flight speed v for optimum momentum transfer.

The Yarkovsky force is most significant for approximately meter to decameter scales – i.e., meteorites and asteroid fragments. The force is reduced from its 'ideal' value for small objects, where the distance scale is short enough for some of the dayside heat to be conducted through the object and radiated from the nightside (see e.g., Vokrouhlický 1998). Conventionally this may be viewed as a reduction in the thrust asymmetry, but from the thermodynamic perspective, it is a conductive heat loss that 'shorts out' the rotating heat engine.

It is reassuring that the Yarkovsky effect falls comfortably into the paradigm of a heat engine, although it is not yet clear how thermodynamics may offer new insights that the conventional momentum accounting approaches have not (although, see e.g., Fort et al. 1999 for an entropy treatment of stellar limb-darkening). Nonetheless, it is possible (e.g., Lorenz 2002) that interacting particles such as those in a planetary ring or circumstellar nebula may have degrees of freedom that permit self-organization and optimization of entropy production (see also Sommeria, this volume).

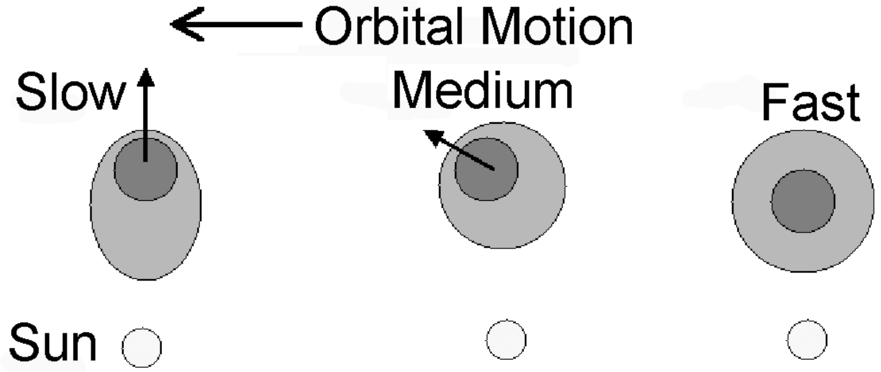

Fig. 12.3. Schematic diagram of the Yarkovsky effect for a spherical asteroid (mid-grey circle) with its rotation axis normal to the orbital plane. For a slow rotator (*left*) the temperature distribution (dark grey ellipse) is in equilibrium with sunlight, with a strong noontime temperature bulge: the thrust from the reradiated thermal radiation is therefore maximized, but is orthogonal to the direction of motion and thus performs no work. A fast rotator (*right*) has a near-isothermal temperature distribution and there is no net photon thrust. At an intermediate rotation rate, the maximum temperature occurs in the afternoon, such that the photon thrust, albeit slightly lower than the maximum at left, has a significant component along the direction of motion and thus the work output is maximized

12.6 Dyson Sphere – The Ultimate Stage in Planetary Evolution

The paradigm of a civilization's ultimate goal as the total downconversion of a star's light into thermal radiation is a neat image of life and order as being driven by thermodynamics and seeking to maximize their entropy production (see also Chaisson, this volume). Freeman Dyson suggested (Dyson 1960) that the presence of an advanced civilization might be revealed by the enhancement of infrared flux from a star. Mass and energy (or more specifically, available energy) are the limiting factors in growth, and Dyson noted that the growth in population and energy use of a civilization is much more rapid than the evolution of a star's luminosity, and thus a growing civilization would want to exploit an ever-larger fraction of the energy being radiated from its parent star. In particular, he notes that an expansion of population and industry of only 1 per cent per year for 3000 years would lead to an increase in energy use by a factor of 10^{12}. The human species presently exploits the mass of the biosphere of 5 10^{16} kg, consuming 10^{13} W. A factor of 10^{12} increase in these quantities corresponds roughly to the maximum mass reasonably accessible to humanity, taken as the mass of the planet Jupiter (2×10^{27} kg) and to the total energy output of the Sun, namely 4×10^{26} W. To exploit this energy output would require both a device for intercepting it (a shell to capture the sunlight) and the rejection of that energy at a lower temperature.

Dyson noted that the mass of Jupiter could be rearranged into a spherical shell at 2 astronomical units from the Sun. The thickness of this shell would be a few meters, depending on the density, and the shell would have an equilibrium temperature about equal to the Earth's present value (although some engineering details such as the heat transport across the shell have not been considered here). Well-behaved stars lie on an evolutionary track on the Hertzsprung-Russell diagram, a plot of luminosity with spectral type. If a star were to be obscured by a Dyson sphere, its emission spectrum would shift to the infrared, compared with stars of similar luminosity.

Although this idea remains interesting as a thought experiment, much recent astronomical work has been devoted to detecting such infrared excess not in order to search for extraterrestrial civilizations, but in order to detect non-artificial opaque envelopes around stars. Specifically, a cloud of dust in a protoplanetary nebula may surround a star, blocking its light but re-emitting its energy as infrared just as would a Dyson sphere. Thus infrared excesses are signals that something interesting is happening around a star, but is not necessarily a signature of astroengineering.

12.7 Concluding Remarks

This chapter surveyed some applications of nonequilibrium thermodynamics in the planetary sciences. Thermodynamic principles appear of particular utility in situations where there is little real data and thus the study of other planets can benefit from these ideas.

References

Aoki I (1983) Entropy productions on the earth and other planets of solar system, J. Phys. Soc. Jpn., 52, 1075–1078.

Burns JA, Lamy PL, Soter S (1979) Radiation forces on Small Particles in the Solar System, Icarus 40: 1–48.

Conrath B and Gierasch P (1985) Energy Conversion Processes in Outer Planet Atmospheres, in G E Hunt (ed) Recent Advances in Planetary Meteorology, Cambridge University Press, Cambridge, UK.

Dewar RC (2003) Information theory explanation of the fluctuation theorem, maximum entropy production, and self-organized criticality in non-equilibrium stationary states. J Physics A 36: 631–641.

Dyson FJ (1960) Search for Artificial Sources of Infrared Radiation. Science 131: 1667–1668.

Farinella P, Vokrouhlický D, Hartmann W (1998) Meteorite Delivery via Yarkovsky Orbital Drift. Icarus 132: 378–387.

Fort J, Gonzalez J, LLebot J, Saurina J (1999) Information theory and blackbody radiation. Contemporary Physics 40: 57–70.
Goody RM (2000) Sources and sinks of climate entropy. Q J Roy Meteorol Soc 126: 1953–1970.
Kessler MA, Werner BT (2003) Self-Organization of Sorted Patterned Ground. Science 299: 380–383.
Leopold LB, Langbein WB (1962) The Concept of Entropy in Landscape Evolution. U S Geological Survey Professional Paper 500-A.
Lorenz EN (1960) Generation of available potential energy and the intensity of the general circulation. in Pfeffer, RL (ed), Dynamics of Climate, Pergamon, Tarrytown, NY, pp 86–92.
Lorenz RD (2002) Planets, Life and the Production of Entropy. International Journal of Astrobiology 1: 1–13.
Lorenz RD, McKay CP (2003) A Simple Expression for Vertical Convective Fluxes in Planetary Atmospheres. Icarus 165: 407–413.
Lorenz RD, Rennó NO (2002) Work Output of Planetary Atmospheric Engines: Dissipation in Clouds and Rain. Geophys Res Lett 29: 1023, doi:10.1029/2001GL013771.
Lorenz RD, Spitale JN (2004) The Yarkovsky Effect as a Heat Engine. Icarus, 170:229–233.
Lorenz RD, Lunine JI, Withers PG, McKay CP (2001) Titan, Mars and Earth: Entropy production by latitudinal heat transport. Geophys Res Lett 28: 415–418.
Ozawa H, Ohmura A (1997) Thermodynamics of a global-mean state of the atmosphere – A state of maximum entropy increase. J Clim 10: 441–445.
Ozawa H, Ohmura A, Lorenz RD, Pujol T (2003) The Second Law of Thermodynamics and the Global Climate System – A Review. Rev Geophys 41: 1018. doi: 10.1029/2002RG000113.
Paltridge GW (1975) Global dynamics and climate – a system of minimum entropy exchange, Q J R Meteorol Soc 101: 475–484.
Pauluis O, Held IM (2002a) Entropy Budget of an Atmosphere in Radiative–Convective Equilibrium. Part II: Latent Heat Transport and Moist Processes. J Atm Sci 59: 140–150.
Pauluis O, Held IM (2002b) Entropy Budget of an Atmosphere in Radiative–Convective Equilibrium. Part I: Maximum Work and Frictional Dissipation. J Atm Sci 59: 125–139.
Rennò, NO Nash AA, Lunine JI, Murphy J (2000) Martian and terrestrial dust devils: Test of a scaling theory using Pathfinder data. J Geophys Res 105: 1859–1866.
Stephens GL, O'Brien DO (1993) Entropy and climate, I, ERBE observations of the entropy production. Q J Roy Meteorol Soc 119: 121–152.
Vanyo JP, Paltridge GW (1981) A model for energy dissipation at the mantle-core boundary. Geophys J R Astron Soc 66: 677–690.
Verkley, WTM, Gerkema, T (2002) Maximum entropy profiles. J Atm Sci 61:931–936.
Vokrouhlický D (1998) Diurnal Yarkovsky effect as a source of mobility of meter-sized asteroidal fragments. Astronomy and Astrophysics 335: 1093–1100.
Werner BT (1995) Eolian Dunes: Computer Simulations and Attractor Interpretation. Geology 23: 1107–1110.